

# Solving the Jigsaw Puzzle of Wound-Healing Potato Cultivars: Metabolite Profiling and Antioxidant Activity of Polar Extracts

Keyvan Dastmalchi,<sup>†</sup> Qing Cai,<sup>†</sup> Kevin Zhou,<sup>†</sup> Wenlin Huang,<sup>†</sup> Olga Serra,<sup>‡</sup> and Ruth E. Stark<sup>\*,†</sup>

<sup>†</sup>Department of Chemistry, The City College of New York, City University of New York Graduate Center and Institute for Macromolecular Assemblies, New York, New York 10031, United States

<sup>‡</sup>Laboratori del Suro, Departament de Biologia, Facultat de Ciències, University of Girona, Campus Montilivi s/n, Girona E-17071, Spain

## Supporting Information

**ABSTRACT:** Potato (*Solanum tuberosum* L.) is a worldwide food staple, but substantial waste accompanies the cultivation of this crop due to wounding of the outer skin and subsequent unfavorable healing conditions. Motivated by both economic and nutritional considerations, this metabolite profiling study aims to improve understanding of closing layer and wound periderm formation and guide the development of new methods to ensure faster and more complete healing after skin breakage. The polar metabolites of wound-healing tissues from four potato cultivars with differing patterns of tuber skin russeting (Norkotah Russet, Atlantic, Chipeta, and Yukon Gold) were analyzed at three and seven days after wounding, during suberized closing layer formation and nascent wound periderm development, respectively. The polar extracts were assessed using LC-MS and NMR spectroscopic methods, including multivariate analysis and tentative identification of 22 of the 24 biomarkers that discriminate among the cultivars at a given wound-healing time point or between developmental stages. Differences among the metabolites that could be identified from NMR- and MS-derived biomarkers highlight the strengths and limitations of each method, also demonstrating the complementarity of these approaches in terms of assembling a complete molecular picture of the tissue extracts. Both methods revealed that differences among the cultivar metabolite profiles diminish as healing proceeds during the period following wounding. The biomarkers included polyphenolic amines, flavonoid glycosides, phenolic acids and glycoalkaloids. Because wound healing is associated with oxidative stress, the free radical scavenging activities of the extracts from different cultivars were measured at each wounding time point, revealing significantly higher scavenging activity of the Yukon Gold periderm especially after 7 days of wounding.

**KEYWORDS:** *Solanum tuberosum*, closing layer, wound periderm, NMR, LC-MS, biomarkers, antioxidant markers, ABTS<sup>•+</sup> scavenging activity

## ■ INTRODUCTION

The economic importance of potato (*Solanum tuberosum* L.) has grown considerably during the 12 000 years since its domestication and cultivation in the region of Southern Peru and Northern Bolivia around Lake Titicaca,<sup>1,2</sup> bringing it to its current status as a staple crop in many developing and developed countries.<sup>3</sup>

A central challenge faced during cultivation, harvest, and storage of potatoes concerns the wounding of their surfaces and subsequent suboptimal healing conditions that lead to significant crop losses.<sup>4</sup> Thus, it is of considerable commercial and nutritional importance to identify biomarkers that indicate the progress and completeness of healing for wounded surfaces in potato.<sup>5</sup> As a rule, by 1 day after potato tuber wounding, a suberized closing layer begins to form as an initial healing response and by 5–6 days, it is fully developed. During the latter time period the nascent wound phellem layers emerge, signaling the beginning of wound periderm development for both russet and smooth skin genotypes.<sup>5,6</sup> Because the wound-healing response varies with cultivar and species, four different cultivars with distinctive russeting features (Norkotah Russet, Atlantic, Chipeta, and Yukon Gold) (Table 1) were chosen to compare metabolite profiles during closing layer formation and wound periderm initiation, at time points 3 and 7 days after

wounding, respectively. Russeted characteristics are morphological features characterized by rough skin texture and proposed to arise from expansion of the tuber that results in cracking of the skin.<sup>7</sup> Some breeding programs have selected in favor of these traits.<sup>8</sup> The four cultivars selected for study also have contrasting commercial importance: Atlantic and Chipeta are used primarily for processing into potato chips, whereas Norkotah Russet and Yukon Gold are used for baking. The last one is considered to be a leading cultivar because of its high yield, attractive appearance and excellent storability.

Although an increasing number of metabolite profiling reports have appeared for potatoes in recent years,<sup>9–12</sup> the literature on compositional analysis of wound-induced potato tubers<sup>13</sup> and especially polar extracts remains fairly sparse.<sup>13,14</sup> In a study performed by Yang et al.,<sup>14</sup> both polar and nonpolar wound-healing extracts from the Russet Burbank cultivar were analyzed using gas chromatography–mass spectrometry (GC-MS) and metabolomics methods. Nonetheless, extensions of these profiling analyses across cultivars are desirable from both

**Received:** October 21, 2013

**Revised:** June 21, 2014

**Accepted:** July 6, 2014

**Published:** July 7, 2014

Table 1. Potato Cultivars for Wound Healing Study

cultivar	flesh	periderm russetting	skin
Norkotah Russet	white	russeted and netted	dark tan
Atlantic	white	lightly netted to heavily scaled	white
Chipeta	white	small russeted areas	light to buff
Yukon Gold	light yellow	smooth, finely flaked, yellowish white	yellowish

methodological and agricultural standpoints: high performance liquid chromatography (LC-MS) and nuclear magnetic resonance (NMR) may offer more robust characterization of the healing tissue extracts, and cultivar comparisons could show metabolite differences that reveal the molecular underpinnings of russeted skin character and/or wound-induced stress response.

In turn, the oxidative stress due to wounding can unleash the production of antioxidant compounds, which are present in the native skin of potato and have already found practical use as preservatives in the food industry.<sup>3</sup> Antioxidant evaluation of a purple potato cultivar using a diphenyl picrylhydrazyl (DPPH<sup>•</sup>) scavenging assay showed that the activity increased as a result of wounding,<sup>15</sup> but a trend of decreasing DPPH<sup>•</sup> scavenging activity was reported in a wounded Norkotah Russet sample.<sup>16</sup> This inconsistency could reflect a shortcoming of the DPPH<sup>•</sup> assay, whereby steric hindrance could compromise assessments of scavenging activities for larger phytochemical constituents. Thus, the current experimental design couples LC-MS and NMR metabolite profiling for four cultivars, at day 3 and day 7 after wounding, with broadly applicable extended-duration scavenging assays using 2,2'-Azinobis (3-ethylbenzothiazoline-6-sulfonic acid ammonium salt) (ABTS<sup>•+</sup>).<sup>17</sup> By coordinating information on chemical composition and antioxidant activity, the long-term goal is to develop improved methods that ensure rapid and complete wound healing for various potato cultivars while also providing a rich source of chemical compounds with potential application as functional foods.<sup>3,18,19</sup>

## MATERIALS AND METHODS

**Reagents.** HPLC-MS grade acetonitrile, water, chloroform and methanol (J. T. Baker, Phillipsburg, NJ) and formic acid (Sigma-Aldrich, St. Louis, MO) were used for LC-MS/MS and time-of-flight (TOF-MS) analysis. 2,2'-Azinobis (3-ethylbenzothiazoline-6-sulfonic acid ammonium salt) (ABTS), 6-hydroxy-2,5,7,8 tetramethylchromane-2-carboxylic acid (TCl, Tokyo, Japan), and potassium peroxosulfate (Sigma-Aldrich, St. Louis, MO) were utilized in the antioxidant assay.

**Plant Material.** Potato tuber cultivars from the 2011 crop year were provided by Joe Nuñez, University of California Cooperative Extension (Davis, CA). Table 1 summarizes the differences in overall phenotypic characteristics that were used in making these selections.

**Sample Preparation.** Freshly harvested potato tubers were peeled, and the internal flesh tissues were sectioned longitudinally with a mandolin slicer to obtain slices about 5 mm thick. The central part of the tuber was set aside to avoid the internal medulla. Slices were placed on wet cellulose filter paper and left for 3 or 7 days of healing on wire netting supports within closed plastic boxes at 25 °C. Water was added at the bottom of the boxes to maintain humidity; healing proceeded in the dark. The brown surface layer of wound-healing tissue was collected carefully using a flat spatula, making efforts to avoid flesh (parenchyma) contamination. The samples were harvested at 3 and 7 days after wounding, representing the early healing tissue in which the suberized closing layer and the wound periderm were developing, respectively. Harvested wound periderm samples were frozen immediately in liquid nitrogen and stored at -80 °C until processed. For processing, samples were ground under liquid nitrogen, freeze-dried, and again stored at -80 °C.<sup>20</sup>

The samples were prepared for chemical analysis using a modification of the method employed by Choi et al., which enables concurrent extraction and partitioning of polar and nonpolar constituents and has become an established protocol for metabolomic studies of plant materials.<sup>20,21</sup> Samples of 10 mg (dry weight) each were placed in jn glass vials (Microliter Analytical Supplies, Suwanee, GA) and extracted with 2 mL of 60% (v/v) methanol-water by pan ultrasonication (Branson Ultrasonics, Danbury, CT) for 1 min, followed by addition of 2 mL chloroform and sonication again for 1 min. Each extract was then incubated at room temperature in a shaker for 10 min, followed by tabletop centrifugation (Beckman Coulter, Fullerton, CA) at 3000 rpm to produce three separate phases: soluble polar, soluble nonpolar, and an interphase of suspended particulates. Six replicate extracts were prepared per cultivar for each wound-healing time point (day 3 and day 7). The upper soluble polar extracts were removed carefully with a glass Pasteur pipet and dried under a flow of nitrogen for a few hours. This phase was selected for the current analysis.

**NMR.** Aliquots of the polar extract were dried and reconstituted using a 100 mM pH 7.4 phosphate buffer in D<sub>2</sub>O that contained the internal standard DSS (0.01 mg/mL). Spectra were recorded using a Bruker AVANCE PLUS spectrometer (Bruker Biospin, Karlsruhe, Germany) operating at a <sup>1</sup>H frequency of 800 MHz and equipped with a cryomicroprobe that accommodates 1.7 mm o.d. sample tubes (Norell, Landisville, NJ). Acquisition of the spectra was achieved using TOPSPIN version 3.1 software and an NMR SAMPLEJET accessory for automated sample changing. <sup>1</sup>H NMR data were collected for the polar extracts at 298 K with a constant receiver gain, using 512 scans with 4 initial "dummy" scans, a recycle delay of 1.0 s between acquisitions, and presaturation of the residual water signal set to a chemical shift of 4.695 ppm. The spectral window after Fourier transformation and signal conditioning was 14 ppm defined by 32K data points.

**LC-MS.** Liquid chromatography was conducted with a Shimadzu UFLC (Shimadzu U.S.A., Canby, OR) equipped with two LC-20 AD pumps, a SIL-20AC automatic injector, a CBM-20A communication bus module and a CTO-20AC column oven. The separations were carried out using a 150 × 4.6 mm i.d., 3.0 μm AscentisR C18 column (Supelco Analytical, Bellefonte, PA). Each analysis was performed by injecting a 10 μL sample into the column and eluting at 35 °C with a flow rate of 0.4 mL/min. Six replicate extracts per cultivar were analyzed for each wound-healing time point, and each sample was injected twice. The mobile phase was composed of 0.1% aqueous formic acid (A) and 0.1% formic acid in acetonitrile (B) using a program of nonlinear gradient elution: 2% B (0–5 min), 2–10% B (5–8 min), 10–15% B (8–13 min), 15% B (13–25 min), 15–30% B (25–28 min), 30–40% B (28–50 min), and 40–100% B (50–60 min).

The LC system was interfaced to an Applied Biosystems 4000 Q Trap mass spectrometer (Applied Biosystems, Foster City, CA) for LC-MS/MS measurements. The source type was electrospray ionization (ESI) and the source temperature was 300 °C. Mass spectra were acquired in both positive and negative modes over the range *m/z* 100–1300. Full scan, MS<sup>2</sup>, and MS<sup>3</sup> data were collected using these settings. The optimized declustering potentials were 66 V in the positive mode and -140 V in the negative mode; chlorogenic acid and rutin, compounds reported previously in potatoes,<sup>9,11,22</sup> were used as reference standards. Analyst 1.4.2 software was used for data processing.

**Fractionation of the Extracts.** The polar extracts were fractionated using an Agilent 1200 series HPLC-PDA liquid

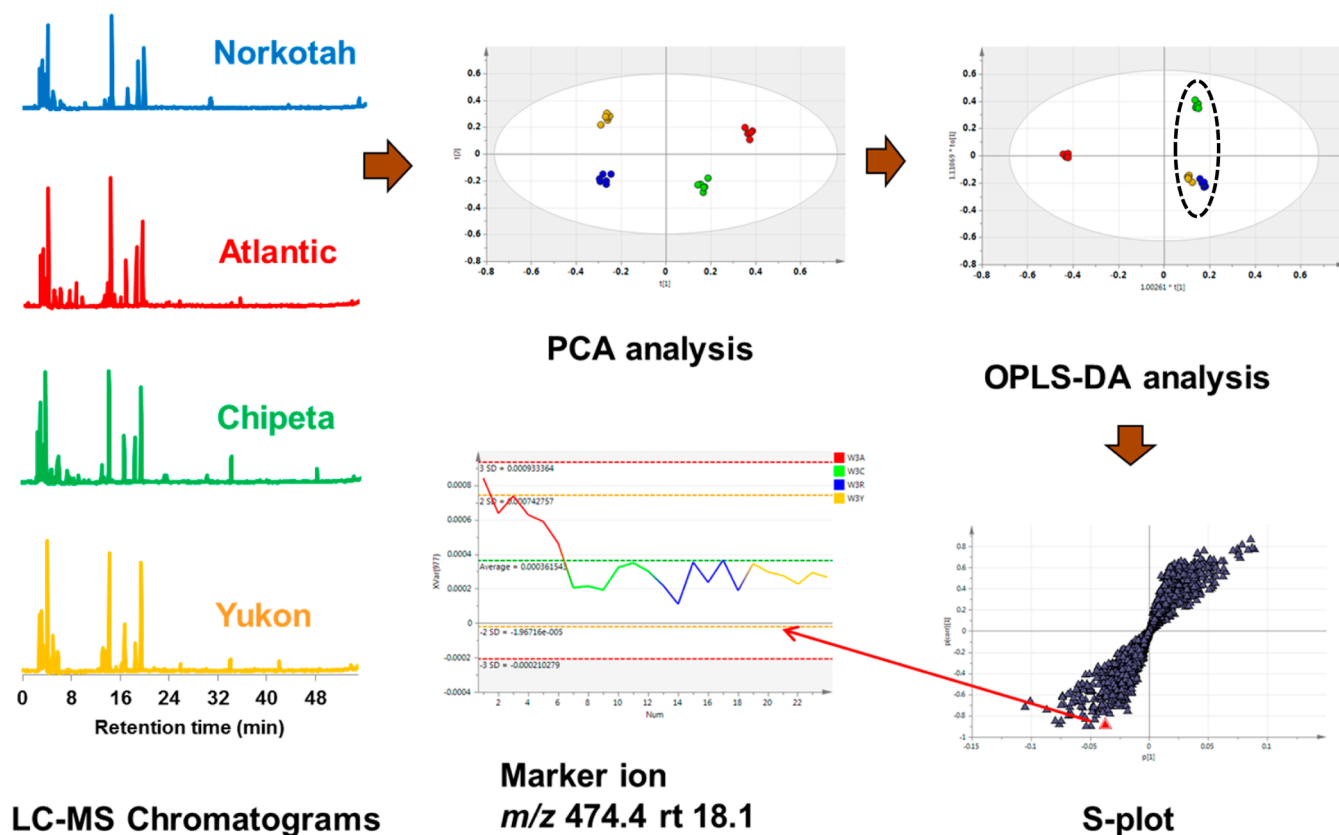


**Figure 1.** Schematic representation of the experimental design, including typical data and statistical multivariate analyses including PCA, OPLS-DA and S-plot analysis of liquid chromatography - mass spectrometry (LC-MS) data (total ion current (TIC) chromatograms in positive mode), leading to the detection of marker ions. Stacked LC-MS chromatograms of the polar extracts each represent average data from six biological replicates from day 3 potato wound periderm samples, color coded for Norkotah Russet (blue), Atlantic (red), Chipeta (green), and Yukon Gold (gold). Statistical procedures are detailed in the text.

chromatography system (Agilent Technologies, Santa Clara, CA) equipped with a G1322A degasser, G1311A quaternary pump, G1316A thermostatically controlled chamber, G1315B diode array detector, and G1364C analytical fractionator. The mobile phase composition, flow rate, gradient, and column were as described above. Fractions were collected at 30-s intervals throughout a 60 min chromatographic run. This fractionation protocol was repeated several times to generate sufficient material that could be concentrated and analyzed by TOF-MS to obtain the exact mass of the compounds under investigation.

**TOF-MS.** Chromatographic fractions from the polar extracts were injected directly into a Waters LCT premier XE TOF mass spectrometer (Micromass, Manchester, U.K.) using a Harvard 11 Plus Single Syringe Pump (Harvard Apparatus, Holliston, MA) equipped with an ESI interface and controlled by MassLynx V4.1 software. Mass spectra were acquired in both positive and negative modes over the range  $m/z$  100–1300. The capillary voltages were set at 4000 V for both acquisition modes. Nitrogen gas flowing at 300 L/h was used for both the nebulizer and in desolvation. The desolvation temperature was 150 °C, and the source temperature was 80 °C. For the dynamic range enhancement (DRE) lockmass, a solution of leucine enkephalin (Sigma-Aldrich, St. Louis, MO) was infused by a secondary reference probe at 200 pg/mL in acetonitrile/water (1:1 v/v) containing 0.1% formic acid with the help of a second LC pump (Waters 515 HPLC). The reference mass was determined once every five scans for both positive and negative data collection; both types of ESI data were collected using a scan time of 0.2 s and an interscan time of 0.01 s.

**ABTS<sup>•+</sup> Scavenging.** The ABTS<sup>•+</sup> scavenging activity was assessed according to the method described by Re et al.<sup>17</sup> with minor modifications. ABTS<sup>•+</sup> was generated by reacting an aqueous ABTS

solution (7 mM) with  $K_2S_2O_8$  (2.45 mM) in the dark for 12–16 h at ambient temperature and adjusting the absorbance at 734 nm to 0.70 ( $\pm 0.02$ ) with ethanol. To a 2  $\mu$ L aliquot of the periderm extract of interest was added 198  $\mu$ L of ABTS<sup>•+</sup> reagent; the absorbance was recorded at 734 nm after initial mixing and subsequently at 5 min intervals (45 min in total) using a Spectra<sub>max</sub> microplate reader (Molecular Devices, Sunnyvale, CA). The percentage inhibition values for different concentrations were calculated using the following equation:

$$\left[ \frac{(\text{Abs}_{\text{control}}) - (\text{Abs}_{\text{sample}})}{(\text{Abs}_{\text{control}})} \right] \times 100 \quad (1)$$

A plot of percentage inhibition versus concentration was made for the reference standard, 6-Hydroxy-2,5,7,8-tetramethylchroman-2-carboxylic acid (Trolox). On the basis of this plot, the Trolox equivalent antioxidant capacity (TEAC,  $\mu$ mol Trolox/g dried sample) values were calculated for each extract.

**Preprocessing of NMR Data.** For metabolite profiling analysis, MESTREC software version 4.9.9.9 (Mestrelab Research, Escondido, CA) was used to correct the phase and baseline of each spectrum and to remove the spectral region containing the remaining water signal. The spectra were then subjected to binning and integrated in 0.04 ppm regions. The integrated area of each bin/bucket was normalized with respect to the area of all bins.

**Preprocessing of LC-MS Data.** MZmine version 2.4 (VTT Technical Research Center, Helsinki, Finland and Turku Center for Biotechnology, Turku, Finland) was used to filter the spectra according to retention time and  $m/z$  range. Spectral deconvolution and feature detection were followed by peak alignment and data normalization.<sup>23</sup> The region of the chromatogram between 0 and 4

Table 2. Biomarkers for Polar Extracts of Wound-Healing Potato Periderms

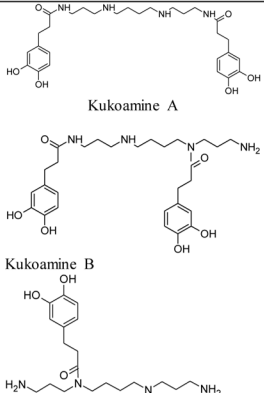
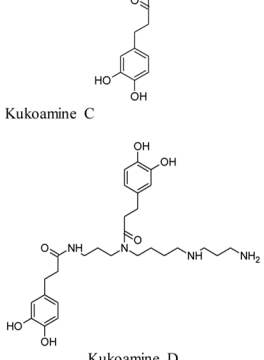
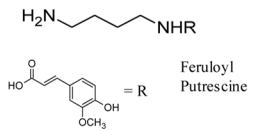
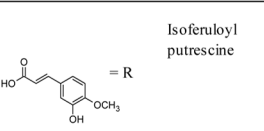
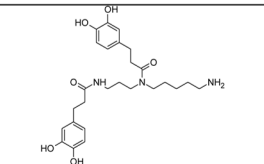
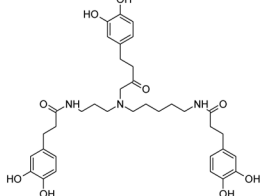
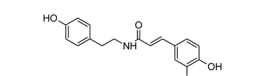
Compound No.	[M+H] <sup>+</sup> or [M+Na] <sup>+</sup> ions exact masses (formula, error) <sup>a</sup>	MS/MS Fragment ions (positive mode) ( <i>m/z</i> ) <sup>b</sup>	Biomarker Formula and Molecular Weight	Structural Formula	Cultivar-Specific Marker <sup>c</sup>	Day 7 Time-Point Marker <sup>f</sup>	References
<b>Identified Constituents</b>							
<b>Phenolic amines</b>							
1	531.3167 [M+H] <sup>+</sup> (C <sub>28</sub> H <sub>43</sub> N <sub>4</sub> O <sub>6</sub> -3.0ppm)	413, 367, 310 266, 257, 222, 184, 165, 123	<b>Kukoamine isomer</b> <i>N,N</i> -bis (dihydrocaffeoyl) spermine C <sub>28</sub> H <sub>42</sub> N <sub>4</sub> O <sub>6</sub> <sup>c,d</sup> 530.3104		Atlantic (Wd3) Norkotah Russet (Wd3)	+	10, 11, 45
2	531.3180 [M+H] <sup>+</sup> (C <sub>28</sub> H <sub>43</sub> N <sub>4</sub> O <sub>6</sub> 0.6ppm)	413, 367, 310 266, 257, 222, 184, 165, 123	<b>Kukoamine isomer</b> C <sub>28</sub> H <sub>42</sub> N <sub>4</sub> O <sub>6</sub> <sup>c,d</sup> 530.3104		Atlantic (Wd3) Norkotah Russet (Wd3)		10, 11
3	265.1534 [M+H] <sup>+</sup> (C <sub>14</sub> H <sub>21</sub> N <sub>2</sub> O <sub>3</sub> -6.8ppm)	162, 149, 134, 117	<b>Feruloyl putrescine</b> C <sub>14</sub> H <sub>20</sub> N <sub>2</sub> O <sub>3</sub> <sup>c,d</sup> 264.1474		Atlantic (Wd3) Yukon (Wd7)		10, 45, 46
4	265.1553 [M+H] <sup>+</sup> (C <sub>14</sub> H <sub>21</sub> N <sub>2</sub> O <sub>3</sub> 0.4ppm)	162, 149, 134, 117	<b>Feruloyl putrescine isomer</b> C <sub>14</sub> H <sub>20</sub> N <sub>2</sub> O <sub>3</sub> <sup>c,d</sup> 264.1474		Atlantic (Wd3) Norkotah Russet (Wd3)	+	10, 46
5	474.2582 [M+H] <sup>+</sup> (C <sub>25</sub> H <sub>36</sub> N <sub>3</sub> O <sub>6</sub> -4.6ppm)	457, 293, 236, 222, 165, 137, 123	<b>N<sup>1</sup>,N<sup>4</sup>-bis (dihydrocaffeoyl) spermidine</b> C <sub>25</sub> H <sub>35</sub> N <sub>3</sub> O <sub>6</sub> 473.2526		Atlantic (Wd3)	+	10, 11, 45
6	638.3086 [M+H] <sup>+</sup> (C <sub>34</sub> H <sub>44</sub> N <sub>3</sub> O <sub>9</sub> 1.3ppm)	474, 293, 236, 222, 165, 137, 123	<b>N<sup>1</sup>,N<sup>4</sup>,N<sup>8</sup>-tris(dihydrocaffeoyl) spermidine</b> C <sub>34</sub> H <sub>43</sub> N <sub>3</sub> O <sub>9</sub> 637.2999		Norkotah Russet (Wd3) Atlantic (Wr3) Chipeta (Wd7)		10, 11
7	314.1386 [M+H] <sup>+</sup> (C <sub>18</sub> H <sub>20</sub> NO <sub>4</sub> -1.9ppm)	177, 159, 149, 145, 134, 125, 121, 117	<b>Feruloyl tyramine</b> C <sub>18</sub> H <sub>19</sub> NO <sub>4</sub> <sup>c</sup> 313.1392		Norkotah Russet (Wd3, Wd7)		11, 24, 26

Table 2. continued

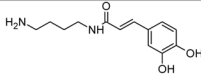
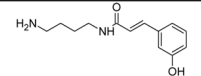
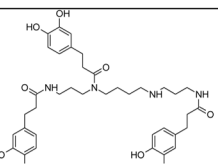
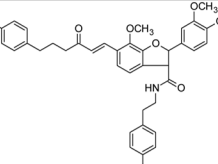
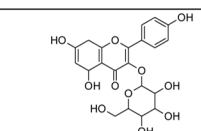
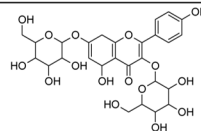
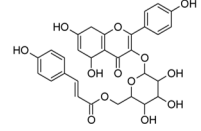
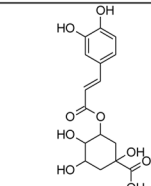
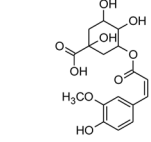
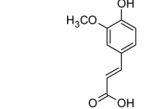
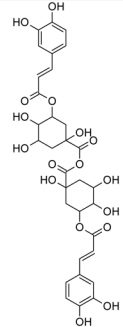
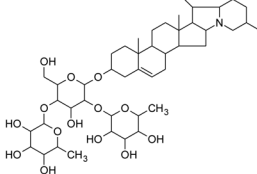
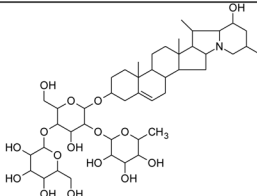
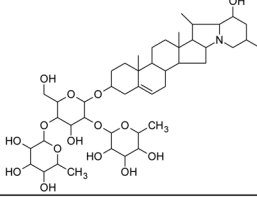
Compound No.	[M+H] <sup>+</sup> or [M+Na] <sup>+</sup> ions exact masses (formula, error) <sup>a</sup>	MS/MS Fragment ions (positive mode) ( <i>m/z</i> ) <sup>b</sup>	Biomarker Formula and Molecular Weight	Structural Formula	Cultivar-Specific Marker <sup>c</sup>	Day 7 Time-Point Marker <sup>d</sup>	References
<b>Identified Constituents</b>							
<b>Phenolic amines</b>							
8	251.1398 [M+H] <sup>+</sup> (C <sub>13</sub> H <sub>19</sub> N <sub>2</sub> O <sub>3</sub> 0.8ppm)	235, 175, 163, 145, 135, 117	<b>Caffeoyl putrescine</b> C <sub>13</sub> H <sub>18</sub> N <sub>2</sub> O <sub>3</sub> 250.1317		Atlantic (Wd3)		10,11
9	235.1471 [M+H] <sup>+</sup> (C <sub>13</sub> H <sub>19</sub> N <sub>2</sub> O <sub>2</sub> 10.2ppm)	218, 179, 147, 119	<b>Coumaryl putrescine</b> C <sub>13</sub> H <sub>18</sub> N <sub>2</sub> O <sub>2</sub> 235.134		Atlantic (Wd7) Chipeta (Wd7)		11
10	695.3613 [M+H] <sup>+</sup> (C <sub>37</sub> H <sub>51</sub> N <sub>4</sub> O <sub>9</sub> 6.2ppm)	677, 531, 457, 386, 293, 276, 222, 165, 123	<b>N<sup>1</sup>,N<sup>3</sup>,N<sup>5</sup>,N<sup>7</sup>-tris(dihydrocaffeoyl) spermine</b> C <sub>37</sub> H <sub>50</sub> N <sub>4</sub> O <sub>9</sub> <sup>e</sup> 694.3578		Norkotah Russet (Wd7) Yukon (Wd7)		10,11
11	625.2567 [M+H] <sup>+</sup> (C <sub>36</sub> H <sub>37</sub> N <sub>2</sub> O <sub>8</sub> 2.7ppm)	488, 460, 351, 323, 308, 291, 265, 250, 237, 201, 191	<b>Grossamide</b> C <sub>36</sub> H <sub>36</sub> N <sub>2</sub> O <sub>8</sub> <sup>f</sup> 624.2471			+	24
<b>Flavonoid glycosides</b>							
12	449.1089 [M+H] <sup>+</sup> (C <sub>21</sub> H <sub>21</sub> O <sub>11</sub> 1.1ppm)	413,413, 329,287	<b>Kaempferol hexoside</b> C <sub>21</sub> H <sub>20</sub> O <sub>11</sub> 448.1006		Yukon (Wd3, Wd7)	+	45
13	611.1628 [M+H] <sup>+</sup> (C <sub>27</sub> H <sub>31</sub> O <sub>14</sub> , 2.6ppm)	449, 413, 383, 329, 287	<b>Kaempferol dihexoside</b> C <sub>27</sub> H <sub>30</sub> O <sub>15</sub>		Yukon (Wd3)		9, 12
14	595.1513 [M+H] <sup>+</sup> (C <sub>30</sub> H <sub>27</sub> O <sub>13</sub> , 3.3ppm)	449,431, 413, 359, 329, 290, 287, 270	<b>Potengriffoside</b> C <sub>30</sub> H <sub>26</sub> O <sub>13</sub> 594.1373		Yukon Wd7 Norkotah Russet (Wd3)		27
<b>Phenolic acids</b>							
15	355.1012 [M+H] <sup>+</sup> (C <sub>16</sub> H <sub>19</sub> O <sub>9</sub> -4.8ppm)	215, 163, 145, 135	<b>Chlorogenic acid</b> 3-Caffeoylquinic acid C <sub>16</sub> H <sub>18</sub> O <sub>9</sub> <sup>e</sup> 354.0951		Yukon (Wd3, Wd7) and Norkotah Russet (Wd3, Wd7)	+	9,47-49
16	369.1165 [M+H] <sup>+</sup> (C <sub>17</sub> H <sub>21</sub> O <sub>9</sub> -5.7ppm)	327, 251, 215, 195, 175, 132	<b>Feruloylquinic acid</b> C <sub>17</sub> H <sub>20</sub> O <sub>9</sub> 368.1107		Norkotah Russet (Wd3, Wd7)		11, 45, 50
17	217.0465 [M+Na] <sup>+</sup> (C <sub>10</sub> H <sub>10</sub> O <sub>4</sub> -5.5ppm)	173, 155, 127	<b>Ferulic acid</b> C <sub>10</sub> H <sub>10</sub> O <sub>4</sub> <sup>f</sup> 194.0579		Yukon (Wd3)	+	9



Table 2. continued

Compound No.	[M+H] <sup>+</sup> or [M+Na] <sup>+</sup> ions exact masses (formula, error) <sup>a</sup>	MS/MS Fragment ions (positive mode) ( <i>m/z</i> ) <sup>b</sup>	Biomarker Formula and Molecular Weight	Structural Formula	Cultivar-Specific Marker <sup>c</sup>	Day 7 Time-Point Marker <sup>d</sup>	References
<b>Identified Constituents</b>							
<b>Phenolic acids</b>							
18	691.1805 [M+H] <sup>+</sup> (C <sub>32</sub> H <sub>34</sub> O <sub>17</sub> -10ppm)	377, 355, 195	<b>Caffeoylquinic acid dimer</b> C <sub>32</sub> H <sub>34</sub> O <sub>17</sub> <sup>h</sup> 690.1796		Atlantic (Wd3, Wd7) and Chipeta (Wd3, Wd7)		47
<b>Glycoalkaloids</b>							
19	852.5095 [M+H] <sup>+</sup> (C <sub>45</sub> H <sub>74</sub> NO <sub>14</sub> -1.6ppm)	707, 561, 398, 380, 366	<b>Chaconine</b> C <sub>45</sub> H <sub>73</sub> NO <sub>14</sub> <sup>e</sup> 851.5031		Chipeta (Wd7)	+	9, 12, 51
20	916.4995 [M+H] <sup>+</sup> (C <sub>45</sub> H <sub>74</sub> NO <sub>18</sub> -9.7ppm) 938.4602 [M+Na] <sup>+</sup> (C <sub>45</sub> H <sub>73</sub> NO <sub>18</sub> Na +13.1ppm)	894, 852, 834, 818, 734, 707	<b>Solanidene triol Solatriose</b> C <sub>45</sub> H <sub>73</sub> NO <sub>18</sub> 915.4828	(structure not reported)	Chipeta (Wd3)		12
21	884.4924 [M+H] <sup>+</sup> (C <sub>45</sub> H <sub>74</sub> NO <sub>16</sub> -9.2ppm)	866, 738, 720, 704, 414, 396, 380, 378, 253	<b>Leptinine II</b> C <sub>45</sub> H <sub>73</sub> NO <sub>16</sub> 883.4929		Norkotah Russet (Wd3)		12
22	868.4992 [M+H] <sup>+</sup> (C <sub>45</sub> H <sub>74</sub> NO <sub>15</sub> -7.6ppm)	850, 722, 704, 558, 414, 396, 378, 253	<b>Leptinine I</b> C <sub>45</sub> H <sub>73</sub> NO <sub>15</sub> 867.4980			+	12
<b>Incompletely Identified Constituents</b>							
23	527.2870	253, 236, 165, 123	Spermine derivative		Yukon Gold (Wd3, Wd7)	+	
24	486.4414	222, 177, 165, 123, 117			Chipeta (Wd7)		

<sup>a</sup>Exact mass data obtained from MS-TOF analysis. <sup>b</sup>Fragmentation data obtained from LC-MS/MS analysis using a 4000Q Trap instrument. <sup>c</sup>Also among the biomarkers identified in native periderms of these four cultivars (Huang et al., unpublished observations). <sup>d</sup>Isomeric compounds which were distinguished from each other by their retention times and the intensities of their mass fragmentation peaks. <sup>e</sup>The wound healing time point is denoted by Wd3 or Wd7, and color coded depending on the cultivar(s) specific for the biomarker. The coloring scheme denotes Atlantic (red), Chipeta (green), Norkotah Russet (blue), or Yukon Gold (gold). <sup>f</sup>Marker compounds found in all four cultivars that are specific to day 7 post wounding, which is associated with nascent wound periderm development. The (+) sign indicates that the compound in question is a marker for the day 7 time point. <sup>g</sup>Also among the metabolites identified in native periderms of these four cultivars (Huang et al., unpublished observations). <sup>h</sup>This compound can be distinguished from gas-phase dimer ions produced as artifacts during MS analysis: the observed *m/z* value of its molecular ion differs from a simple doubling of chlorogenic acid due to loss of water consequent with dimer formation.

min, which contains primary metabolites reported previously,<sup>14</sup> was not included in the current PCA analysis.

**Multivariate Data Analysis.** Principal component analysis (PCA) of the normalized data from NMR and MS experiments was carried

out using Simca-P+ software version 13.0 (Umetrics, Umeå, Sweden) and Pareto scaling.<sup>20</sup> In addition, the data were subjected to orthogonal partial least-squares discriminate analysis (OPLS-DA), in which data from a particular cultivar were assigned to one class that was then compared with another class comprising the remaining cultivars. The corresponding S-plots displayed extreme “wings” that yielded chemical shifts or mass-to-charge ( $m/z$ ) ratios of the biomarkers that contribute to compositional differences among the tissue samples (Figure 1). These variables were evaluated individually using variable line plots to ascertain if the markers were unique to a particular cultivar at a specified wounding time point (Figure 1).

**Tentative Metabolite Structural Identification.** The markers were then characterized using mass and fragmentation data (MS, MS/MS and MS/MS/MS) from the 4000Q Trap and the exact mass values from the TOF-MS instrument, respectively. The marker compounds were identified tentatively by comparison of these data with published MS results using SciFinder Scholar and online databases such as PubChem, ChemSpider and Metlin.

To check the consistency of the MS-based identifications with observed NMR data for the extract mixtures, ACD software (ACD Laboratories, Toronto, Canada) was first used to simulate the NMR spectra of the identified markers. The simulated  $^1\text{H}$  spectra of each compound were checked against the chemical shift list derived for biomarkers by OPLS-DA and S-plot analysis of the experimental NMR data for extract mixtures. For example, a biomarker compound for the Atlantic day 3 extract was tentatively identified as bis (dihydrocaffeoyl) spermidine, compound 5, (474.4  $m/z$ ; 18.1 min) (Figure 1 and Table 2). The simulated  $^1\text{H}$  chemical shifts for this MS-derived biomarker were compared with marker shifts derived from the experimentally observed NMR data for the extract mixture.

## RESULTS AND DISCUSSION

**Metabolic Fingerprinting.** Visual inspection of the stacked  $^1\text{H}$  NMR spectra for wound-healing tissue extracts from various cultivars at days 3 and 7 (Figure 2 and Supporting Information (SI) Figure S1, respectively) shows good consistency among the six replicates for each cultivar, a high

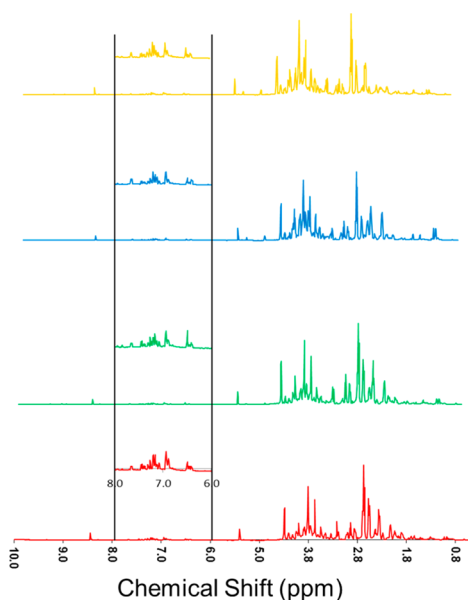


**Figure 2.** Stacked 800 MHz  $^1\text{H}$  nuclear magnetic resonance (NMR) spectra, showing average data from six biological replicates of polar extracts from day 3 potato wound periderm samples, color coded for Yukon Gold (gold), Norkotah Russet (blue), Chipeta (green), and Atlantic (red). Vertical expansions of the aromatic and multiple-bonded region between 6.0 and 8.0 ppm are shown in each inset.

degree of instrumental reproducibility, and modest but clear differences among the four cultivars. A more rigorous multivariate analysis of the data provides essential unbiased confirmation of these differences. The PCA-associated score plots for the NMR data (Figure 3) demonstrate that the polar

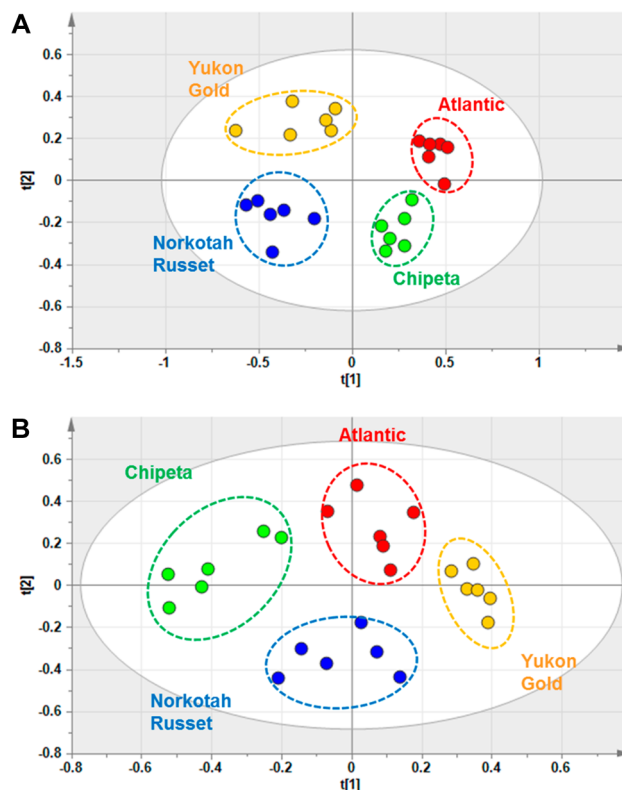


**Figure 3.** PCA score plots for the NMR data from extracts of day 3 (A) and day 7 (B) wound-healing samples, color coded for Atlantic (red), Chipeta (green), Norkotah Russet (blue), and Yukon Gold (gold) potato periderms.

metabolites for each of the four cultivars form distinct and nonoverlapping clusters, more distinct at day 3 compared with day 7 post wounding. To compare the metabolic profiles at different wound-healing time points, PCA was carried out for day-3 and day-7 NMR data together; the resulting score plot (Figure 4) shows a clear separation of metabolites at the two time points according to PC1. Again, a closer convergence of the clusters for each cultivar is evident at day 7.

In an analogous fashion, Figure 2 and SI Figure S2 demonstrate consistency among LC-MS experiments on nominally identical samples and distinct signatures for each of the four cultivars and wound-healing time points. Even more definitively than via NMR data, score plots obtained from PCA analysis of the LC-MS experiments show polar metabolite differences among the clusters corresponding to Russet Norkotah, Atlantic, Chipeta, and Yukon Gold cultivars (Figure 5). As compared with day 3 (Figure 5A), the convergent trend of metabolite compositions at day 7 is demonstrated by both the LC-MS score plot (Figure 5B) and the overall PCA analysis for both healing time points (Figure 6), again aligning with the NMR-derived multivariate analysis (Figures 3 and 4). This convergence of metabolite profiles with time, which has been observed previously in GC-MS-based multivariate analysis of Russet Burbank periderms,<sup>14</sup> could reflect common biosynthetic pathways associated with wounding in the four cultivars.

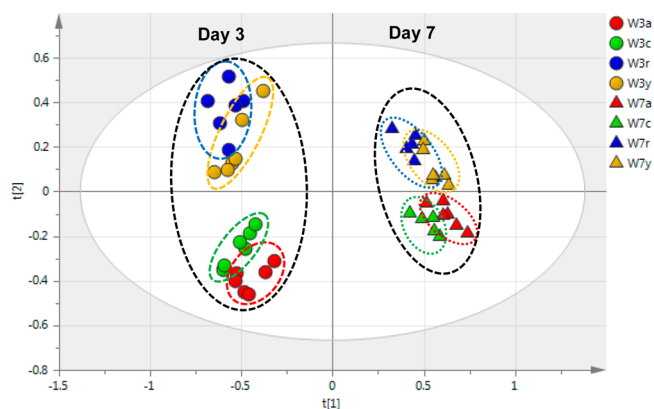


**Figure 4.** PCA score plot for the overall NMR data from extracts of the four cultivars at both day 3 (circles) and day 7 (triangles) post wounding (W). The samples are coded for Atlantic (red, a), Chipeta (green, c), Norkotah Russet (blue, r), and Yukon Gold (gold, y).

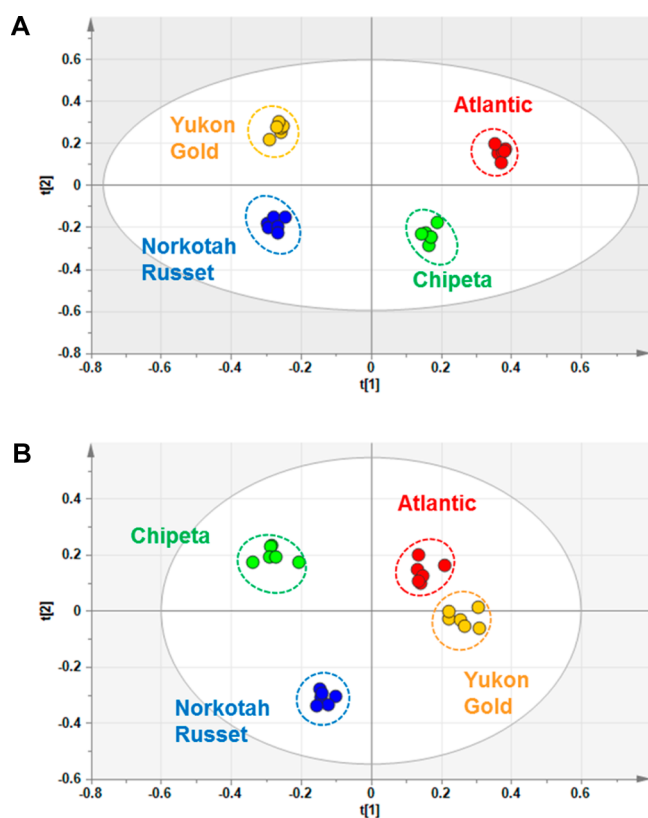


**Figure 5.** PCA score plots for the LC-MS data from extracts of day 3 (A) and day 7 (B) potato wound-healing samples, color coded for Atlantic (red), Chipeta (green), Norkotah Russet (blue), and Yukon Gold (gold).

That is, if the initially distinct metabolite pools for the four cultivars accumulate a common set of phytochemicals associated with wound induction, these common metabolites will become increasingly dominant at later healing stages.

OPLS-DA analyses and their corresponding S-plots, illustrated in Figure 1, provide chemical insight into the basis for variations in metabolic profiles. In particular, it is possible to identify the NMR chemical shifts and/or MS ions corresponding to metabolites (“biomarkers”) that accumulate or are specific for a particular cultivar or wound-healing time point from the extremes of the S-plots. By comparing the marker ions

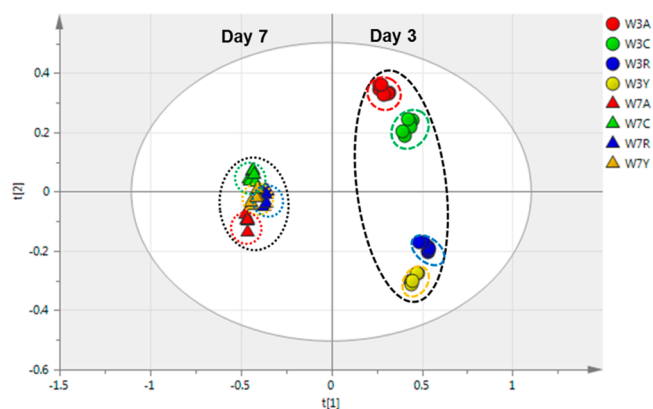


**Figure 6.** PCA score plot for the overall LC-MS data from extracts of the cultivars at both day 3 (circles) and day 7 (triangles) post wounding (W). The periderm samples are coded for Atlantic (red, a), Chipeta (green, c), Norkotah Russet (blue, r), and Yukon Gold (gold, y).

with published MS data using SciFinder Scholar (<https://scifinder.cas.org/scifinder>) or other online databases, it was possible to tentatively identify the polyphenolic amines, flavonoid glycosides, phenolic acids, and glycoalkaloids listed in Table 2. A total of 22 of 24 biomarkers were identified by MS/MS and MS-TOF methods. As noted in the Materials and Methods section, early eluting primary metabolites were excluded from the current PCA analysis.

**Biomarkers for Cultivar Type.** The majority of the identified biomarkers for Atlantic and Norkotah Russet varieties, at both days 3 and 7 post wounding, are polyphenolic amines. Conversely, most of the polyphenolic amine biomarkers are found in the Atlantic and Norkotah Russet cultivars (Table 2). Polyphenolic amines have been claimed previously to offer resistance to potato pathogens such as *Phytophthora infestans* and *Streptomyces scabies*.<sup>24–26</sup> Therefore, accumulation of these antimicrobial compounds can offer protection at the wound site and aid in development of an effective moisture barrier.

The polyphenolic amine biomarkers include derivatives of spermine, spermidine, tyramine, and putrescine. Among these compounds, markers for closing layer formation include kukoamine isomers (1, 2), feruloyl putrescine and its isomer (3, 4),  $N^1, N^4$ -bis (dihydrocaffeoyl) spermidine (5),  $N^1, N^4, N^8$ -tris (dihydrocaffeoyl) spermidine (6), feruloyl tyramine (7) and caffeoyl putrescine (8) for the Atlantic and/or Norkotah Russet cultivars.<sup>24</sup> By contrast, other phenolic amines are found as biomarkers for these cultivars only after the closing layer has been formed and wound periderm formation has been initiated: coumaryl putrescine (9) for Atlantic and  $N^1, N^4, N^{12}$  tris-(dihydrocaffeoyl)spermine (10) for Norkotah Russet, respectively. Feruloyl tyramine (7) is a Norkotah Russet marker at both day 3 and day 7 time points. Compounds 6, 9, and 10 are also markers for the day 7 wound-healing time point in Chipeta or Yukon Gold cultivars. The polyphenolic amine biomarkers listed in Table 2 have been reported previously in the flesh of potato tubers.<sup>10,11</sup> Feruloyl tyramine and related compounds are associated with the lesions and heavier skins formed by scab-infected potato tubers.<sup>24,26</sup> (The phenolic amine Grossamide (11), which is not a cultivar marker but is upregulated for all four cultivars, is discussed in the following section.) One additional unidentified biomarker (23) can be classified as a spermine derivative from its MS data. Finally, several of the



polyphenolic amines in Table 2 were also identified in native periderms (tuber skin) from these four potato cultivars (noted as <sup>a</sup> for biomarkers, <sup>c</sup> for nonbiomarker metabolites; Huang et al., unpublished observations).

Kaempferol glycosides (**12**–**14**) are detected as biomarkers for Norkotah Russet and Yukon Gold. Most of the glycosides are present in Yukon Gold. All glycoside compounds have been reported in potato peels<sup>9</sup> with the exception of Potengriffioside (**14**), which was isolated from *Solanum crinitum* Lam. tubers.<sup>27</sup> One common potato phenolic metabolite that is identified as a biomarker for Yukon Gold and Norkotah Russet is chlorogenic acid (**15**). Feruloyl quinic acid (**16**) is a marker specific to Norkotah Russet at days 3 and 7; ferulic acid itself (**17**), which plays an integral role in suberin formation,<sup>28,29</sup> is a marker for the day 3 extracts of Yukon Gold. Both **15** and **17** have been reported previously in the polar extracts from wound-healing Russet Burbank potato periderms.<sup>14</sup> Finally, the Atlantic and Chipeta cultivars exhibit a caffeoylquinic acid dimer biomarker (**18**) in both 3- and 7-day wound-healing samples.

Glycoalkaloids, compounds **19**–**22**, are identified as biomarkers for Chipeta and Norkotah Russet cultivars. Chaconine (**19**) and solanidine solatriose (**20**) are detected in day 3 and day 7 Chipeta samples, respectively, whereas Leptinine II (**21**) is a marker for day 3 Norkotah Russet polar extracts. Leptinine I (**22**) is a marker for day 7 extracts in all four cultivars and should thus be viewed as a marker associated with this later time point of wound-induced healing. The glycoalkaloids chaconine, leptinine II, leptinine I, and solanidine solatriose have been reported previously in the tubers of Norkotah Russet potatoes.<sup>12</sup> Chaconine has also been reported to be present in potato peels of diverse cultivars.<sup>9,12</sup> Taken together, the glycoalkaloid compounds are viewed as an important class of potato biomarkers because of their demonstrated role in resistance to pests and pathogens.<sup>30</sup> However, they also show concentration-dependent toxicity in organisms ranging from fungi to humans.<sup>31,32</sup> Due to their structural similarity to steroidal hormones, glycoalkaloids are considered additionally to be promising intermediates in the production of contraceptives and steroidal anti-inflammatory drugs.<sup>3</sup> Glycoalkaloids have been reported to have a wide range of bioactivities, including anticancer, anti-inflammatory, antinociceptive, and antipyretic effects.<sup>32</sup>

**Biomarkers for Wound-Healing Time Point.** Although the current comparisons are limited to day-3 and day-7 time points, a prior extended time course study of healing Russet Burbank tubers reported a significantly different polar metabolic profile at day 0, the onset of wound induction.<sup>14</sup> OPLS-DA and S-plot analysis of day-3 and day-7 wound-induced metabolite data for the four cultivars permits the identification of compounds that are more abundant at day 7, the healing time point related to the development of the nascent wound-healing periderm.<sup>5,6</sup> These compounds include several classes of phytochemical substances: polyphenolic amines, flavonoid glycosides, phenolic acids and glycoalkaloids. A kukoamine isomer (**1**), feruloyl putrescine isomer (**4**), *N*<sup>1</sup>,*N*<sup>4</sup> bis(dihydrocaffeoyl) spermidine (**5**), grossamide (**11**), kaempferol hexoside (**12**), chlorogenic acid (**15**), ferulic acid (**17**), chaconine (**19**) leptinine I (**22**), spermine derivative (**23**) were all identified as markers specific to the day-7 healing time point. Thus, compounds produced in significantly larger quantities at the day-7 time point compared with day 3 can be associated with wound periderm development. Indeed, phenolic amines and glycoalkaloids similar to **1**, **4**, **5**, **11**, **19**,

and **22** have been reported to offer resistance against microbes, insects, and herbivores.<sup>25,33</sup> Therefore, their accumulation during wound periderm formation could be part of the protective mechanism against infections.

The current results complement a prior GC-MS study of wound-healing samples from Russet Burbank potato periderms, in which the majority of the identified constituents were primary metabolites but phenolic compounds such as chlorogenic acid, ferulic acid, *iso*-chlorogenic acid, caffeic acid, and coniferyl alcohol were also reported.<sup>14</sup> No phenolic amines, flavonoid glycosides, or glycoalkaloids were identified in the earlier work, presumably because silylation produced species that exceeded the detectable *m/z* ratio, were only partially derivatized, or underwent side reactions rather than the desired formation of volatile derivatives.<sup>34</sup>

**Methodological Challenges for Biomarker Identification.** As shown in Figures 3–6, robust multivariate analyses can be conducted for polar periderm extracts using either NMR or LC-MS data; chemical shifts and mass-to-charge ratios of markers for cultivar type or wound-healing time point can also be extracted from S-plots in OPLS-DA analyses (Figure 1). For each of the 22 MS-derived biomarkers identified by comparison with published mass spectral data (TOF, LC-MS, and mass fragmentation) for potatoes or related plant species, we were able to simulate an NMR spectrum; the prediction could then be cross-checked against biomarker chemical shifts that had been determined from the wings of the corresponding NMR-derived S-plots. This situation is illustrated by the biomarkers for the Yukon Gold day 7 extract: for feruloyl putrescine (**3**), *N*<sup>1</sup>,*N*<sup>4</sup>,*N*<sup>12</sup> tris(dihydrocaffeoyl) spermine (**10**), kaempferol hexoside (**12**), potengriffioside (**14**), and chlorogenic acid (**15**), the MS-based identifications and associated NMR spectral simulations were supported by observed biomarker chemical shifts (e.g., 7.68, 7.48, 7.44, 7.32, 7.28, 7.20, 7.16, 7.04, 7.00, 6.96, 6.88, 6.84, 6.76, 6.72, 6.60, 6.56, 6.52, 6.40, 5.32, 4.26, 4.22, 3.90, 3.86, 3.82, 3.70, 3.38, 3.34, 3.30, 3.10, 2.22, 1.54, and 1.14 ppm).

For biomarkers such as **23**, however, the MS ion could not be identified because no published literature was available; it was possible to deduce its compound class from the associated MS<sup>*n*</sup> fragments and to validate that supposition from the NMR-derived biomarkers. Such novel compounds then remain to be isolated and elucidated using standard but lengthy spectroscopic procedures. Even more seriously, LC-MS could miss an oligomeric biomarker i.e., give a false negative result, if the compound fails to ionize and thus goes undetected. Either previously unreported MS marker ions or biomarkers that do not ionize in MS experiments should be evident if analysis of the NMR data reveals marker shifts that fail to match the predictions for MS-identified compounds.

Although <sup>1</sup>H NMR methods have a broader detection range,<sup>35</sup> they suffer from considerably lower molar sensitivity than MS. A pitfall associated with this limitation is illustrated by the observed marker shifts at 5.40 and 5.44 ppm, which are consistent with NMR spectra predicted for the leptinine II glycoalkaloid (**21**), a metabolite that is accessible by LC-MS but does not satisfy biomarker criteria for the Yukon Gold day-7 polar periderm extract. The limited sensitivity of NMR could render this compound unobservable in the remaining cultivar samples, producing a false positive among the NMR-derived biomarkers. Finally, NMR-based identification of individual metabolites in an extract mixture is also challenged by incomplete spectral resolution, even when multidimensional

experiments are conducted. Although a number of promising NMR-based metabolomic identification approaches have been proposed in recent years,<sup>36</sup> they remain limited by the complexity of plant extract mixtures and the scope of current structural data libraries.

Complications such as those illustrated above reflect incomplete structural databases for plant-derived materials as well as limited MS ionization and NMR sensitivity capabilities, respectively, arguing for use of a conservative dual-method analysis to improve the completeness of the resulting structural profile for constituent metabolites.

**ABTS<sup>•+</sup> Scavenging Activity of Wound-Healing Extracts.** As noted above, the oxidative stress associated with tuber wounding and the potential of potato-derived antioxidant compounds as food preservatives<sup>3</sup> together motivate quantitative assessments of such compounds in potato cultivar samples. Polar extracts of day 3 and day 7 tissue samples were screened for their free radical scavenging activities. All extracts exhibited scavenging activity, and their activities increased with incubation time (Figures 7 and 8). Thus, it may be deduced

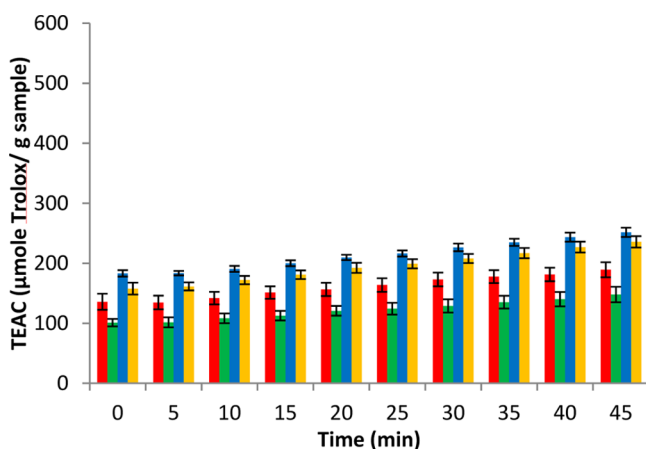


**Figure 7.** ABTS<sup>•+</sup> scavenging activity of polar extracts from day 3 potato wound periderm samples expressed as TEAC ( $\mu\text{mol Trolox/g}$  dried sample), color coded for Atlantic (red), Chipeta (green), Norkotah Russet (blue), and Yukon Gold (gold). Values are expressed as mean  $\pm$  standard error of the mean ( $n = 6$ ). The assay is described fully in the text.

that the cultivars contain slow- as well as fast-acting antioxidants, underscoring the need for an assay such as ABTS<sup>•+</sup> that measures the scavenging capability of the extracts over an extended period of time.<sup>17</sup> The assay has additional advantages such as absence of steric hindrance, a broad pH range, and minimal spectral interference from other natural products,<sup>37,38</sup> distinguishing the current investigation from previous antioxidant research on extracts from potato peels.<sup>15,18,19</sup>

At day 3, the order of activity among the cultivars was as follows: Yukon Gold  $\approx$  Norkotah Russet (not significantly different,  $P > 0.05$ )  $>$  Atlantic  $>$  Chipeta. The order of activity was changed at day 7, to Yukon Gold  $>$  Norkotah Russet  $>$  Atlantic  $>$  Chipeta. Overall, the extracts of Yukon Gold stood out for their high scavenging activity, displaying the highest rates especially after 7 days of wound healing. Although the scavenging capability for most varieties is achieved early during closing layer development and maintained at comparable levels as a functional periderm barrier begins to develop, the Yukon Gold variety nearly doubles its scavenging activity at day 7. This

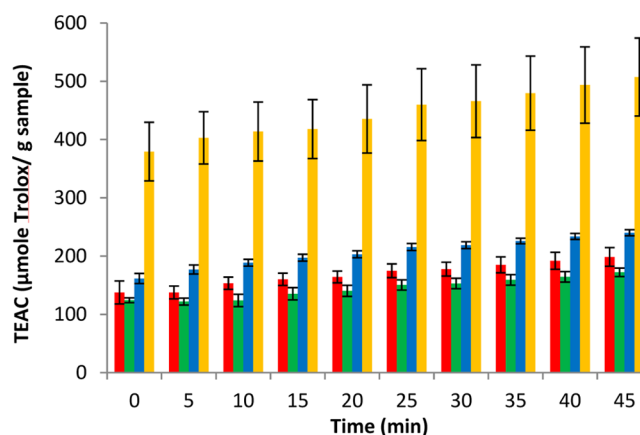


**Figure 8.** ABTS<sup>•+</sup> scavenging activity of polar extracts from day 7 potato wound periderm samples expressed as TEAC ( $\mu\text{mol Trolox/g}$  dried sample), color coded for Atlantic (red), Chipeta (green), Norkotah Russet (blue), and Yukon Gold (gold). Values are expressed as mean  $\pm$  standard error of the mean ( $n = 6$ ). Note that the large standard error of the mean for Yukon day 7 extracts corresponds to a percent error that is similar to the other extracts.

increase in activity could be attributed to the accumulation of antioxidant metabolite(s) during wound periderm development, where the measured extract activity will represent the net effect of potentiation, synergism and antagonism among components of a mixture of antioxidants. The presence of biomarkers such as kaempferol hexoside (12), potengriffioside (14), and chlorogenic acid (15), which have established antioxidant activities,<sup>39,40</sup> could account for the high activity measured in the Yukon Gold extracts. At day 3, extracts of both Yukon Gold and Norkotah Russet demonstrate similar high scavenging activity so that analogously, antioxidant biomarkers such as kaempferol dihexoside (13) potengriffioside (14) chlorogenic acid (15), feruloylquinic acid (16) and ferulic acid (17)<sup>41,42</sup> could be responsible for their robust scavenging activities.

It is also instructive to compare the current antioxidant results with a prior study of unprocessed, baked and chipped tubers from Yukon Gold and Atlantic cultivars. The ABTS<sup>•+</sup> scavenging activities, reported as TEAC values for extracts of those three preparations,<sup>43</sup> were much smaller than values measured herein for both day-3 and day-7 wound-healing tissue extracts from the same cultivars (Table 3). This trend persists even when the previously reported fresh-weight assessments are expressed commensurately to our dry-weight values: the scavenging activities of unprocessed tubers (presumably flesh and skin together) are  $\sim 4$ – $8$  times lower than our late-time point wound sample, for instance. Although a portion of these differences may reflect variations in methodology, the most potent factors are likely to involve our focus on wound-healing tissues and wound induction.

The significantly higher activity observed for the current samples thus supports the potential of wound periderms as sources of antioxidants. Among the studied cultivars, Yukon Gold followed by Norkotah Russet may prove to be of highest value for future industrial applications. Moreover, time-dependent trends in antioxidant assessment can be viewed as a useful tool to monitor the wound-healing process in these potato cultivars.

Table 3. Comparison of ABTS<sup>•+</sup> Scavenging Activities of Tissue Extracts from Atlantic and Yukon Cultivars<sup>a</sup>

cultivar	baked <sup>c</sup>	chipped <sup>c</sup>	unprocessed <sup>c</sup>	dry unprocessed <sup>d</sup>	dry wound periderm day 3	dry wound periderm day 7
Atlantic <sup>b</sup>	1.13 ± 0.12	0.09 ± 0.00	5.75 ± 0.02	57.5	189.28 ± 12.56	198.48 ± 16.01
Yukon Gold	2.30 ± 0.22	0.12 ± 0.00	6.59 ± 0.00	65.9	235.78 ± 9.51	507.38 ± 66.91

<sup>a</sup>The scavenging activities of the samples are expressed as TEAC ( $\mu\text{mol Trolox/g}$  dried sample). <sup>b</sup>The values are expressed as mean  $\pm$  standard error of the mean ( $n = 6$ ). <sup>c</sup>Published TEAC values were measured for tubers. <sup>d</sup>Adjusted by estimating that the tissue is 90%-by-weight water.

## CONCLUSIONS AND PROSPECTUS

The current study is the first report of secondary plant metabolites including phenolic amines, flavonoid glycosides, phenolic acids, and glycoalkaloids as biomarkers for closing layer formation and wound periderm initiation from four potato cultivars with distinctive russeting patterns. Analysis of polar extracts from these materials serves to identify 22 of 24 biomarker compounds that discriminate among the potato cultivars and between healing time points, also revealing the complementary strengths of LC-MS and NMR profiling approaches.

The most heavily russeted Norkotah Russet and Atlantic cultivars are especially rich in polyphenolic amine biomarkers, compounds with established resistance to potato pathogens.<sup>24–26</sup> During suberized closing layer formation (3 days healing), the polyphenolic amine markers are found preferentially in polar periderm extracts from the russeted and netted cultivars, namely Norkotah Russet and Atlantic; that marker class appears at the later day-7 wound-healing time point, if at all, for the smoother Yukon Gold and Chipeta varieties. At the day-7 time point after wound periderm formation has been initiated,<sup>44</sup> both NMR and LC-MS multivariate analyses show significant convergence of the polar metabolite compositions for the four cultivars, suggesting a common wound-healing response which could be compatible with the similar up-regulation patterns reported for cell wall and cell cycle genes during potato tuber wound healing for contrasting potato genotypes and after different harvests.<sup>5</sup> Among the biomarkers for the extracts at day 7, during the formation of the suberized waterproofing barrier, we find polyphenolic amines and glycoalkaloids that are known to confer protection against potato pathogens, pests and herbivores.<sup>25,32</sup> Analysis of the corresponding nonpolar extracts and developing polymeric solids, which can provide complementary information on tissue metabolism after wound induction, will be presented elsewhere.

The presence of antioxidant polyphenolic amine, flavonoid glycoside, and phenolic acid constituents among the biomarkers provides a molecular rationale for the robust radical scavenging activity measured in developing wound periderm extracts from cultivars such as Yukon Gold and Norkotah Russet during wound healing. Nonetheless, the unique rise in day-7 scavenging capability for the Yukon Gold periderm extracts reveals the possible roles of multiple metabolites and the likely interplay of potentiating, synergistic, and antagonistic effects on antioxidant activity. The antioxidants in potato peel have great potential as preservatives in the food industry.<sup>3</sup> As wound periderm formation is initiated, a variety of biomarkers including phenolic amines and glycoalkaloids are found to accumulate; their protective capabilities hold promise for improvements in agricultural productivity.<sup>32,33</sup> In addition glycoalkaloids can be potential intermediates for the production of contraceptive and steroidal anti-inflammatory drugs,<sup>3</sup> and they possess wide ranging bioactivities of interest in drug discovery research.<sup>32</sup> Thus, in addition to the agricultural significance of closing layer and wound periderm formation in

potatoes, the antioxidant and biological activities of the newly identified wounding biomarkers make them potentially interesting to the food and pharmaceutical industries.

## ASSOCIATED CONTENT

### Supporting Information

Figures S1 and S2, overlaid NMR spectra and LC-MS chromatograms of day 7 wound periderm extracts from Norkotah, Atlantic, Chipeta, and Yukon Gold cultivars, respectively. This material is available free of charge via the Internet at <http://pubs.acs.org>.

## AUTHOR INFORMATION

### Corresponding Author

\*Phone: +1 212 650 8916; fax: +1 212 650 8719; e-mail: [rstark@ccny.cuny.edu](mailto:rstark@ccny.cuny.edu).

### Notes

The authors declare no competing financial interest.

## ACKNOWLEDGMENTS

The authors are pleased to acknowledge the New York Structural Biology Center, a STAR center supported by the New York State Office of Science, Technology, and Academic Research and the U.S. National Institutes of Health (2G12 RR03060 from the National Center for Research Resources and 8G12MD007603 from the National Institute on Minority Health and Health Disparities), for providing access to the 800 MHz NMR spectrometer with cryomicroprobe. Dr. Lijia Yang provided expert technical assistance and access to the LC-MS/MS and LC-TOF instruments. Prof. David Jeruzalmi provided generous access to the microplate reader. Joe Nuñez (University of California Cooperative Extension) kindly provided the tubers for these analyses. Financial support for this work came from the U.S. National Science Foundation (MCB-0843627, 1411984, and 0741914 to R.E.S.) and a mobility grant from the Spanish Ministry of Education (JC2010-0147 to O.S.).

## REFERENCES

- Spooner, D. M.; McLean, K.; Ramsay, G.; Waugh, R.; Bryan, G. J. A single domestication for potato based on multilocus amplified fragment length polymorphism genotyping. *Proc. Nat'l. Acad. Sci.* **2005**, *102*, 14694–14699.
- Smith, A. F. *Potato: A Global History*; Reaktion Books: London, 2012.
- Schieber, A.; Saldana, M. D. A. Potato peels: A source of nutritionally and pharmacologically interesting compounds—A review. *Food* **2008**, *3*, 23–29.
- Varns, J. L.; Schaper, L. A.; Preston, D. A. Potato losses during the first three months of storage for processing. *Am. Potato J.* **1985**, *62*, 91–99.
- Neubauer, J. D.; Lulai, E. C.; Thompson, A. L.; Suttle, J. C.; Bolton, M. D. Wounding coordinately induces cell wall protein, cell cycle and pectin methyl esterase genes involved in tuber closing layer and wounding periderm development. *J. Plant Physiol.* **2012**, *169*, 586–595.



- (6) Lulai, E. C.; Corsini, D. L. Differential deposition of suberin phenolic and aliphatic domains and their roles in resistance to infection during potato tuber (*Solanum tuberosum* L.) wound healing. *Physiol. Mol. Plant P.* **1998**, *53*, 209–222.
- (7) Ginzberg, I.; Barel, G.; Ophir, R.; Tzin, E.; Tanami, Z.; Muddarangappa, T.; de Jong, W.; Fogelman, E. Transcriptomic profiling of heat-stress response in potato periderm. *J. Exp. Bot.* **2009**, *60*, 4411–4421.
- (8) Love, S. L.; Werner, B. K.; Pavek, J. J. Selection for individual traits in the early generations of a potato breeding program dedicated to producing cultivars with tubers having long shape and russet skin. *Am. Potato J.* **1997**, *74*, 199–213.
- (9) Ieri, F.; Innocenti, M.; Andrenelli, L.; Vecchio, V.; Mulinacci, N. Rapid HPLC/DAD/MS method to determine phenolic acids, glycoalkaloids and anthocyanins in pigmented potatoes (*Solanum tuberosum* L.) and correlations with variety and geographical origin. *Food Chem.* **2011**, *125*, 750–759.
- (10) Parr, A. J.; Mellon, F. A.; Colquhoun, I. J.; Davis, H. E. Dihydrocaffeoyl polyamines (kukoamine and allies) in potato (*Solanum tuberosum*) tubers detected during metabolite profiling. *J. Agric. Food Chem.* **2005**, *56*, 6949–6958.
- (11) Narvaez-Cuenca, C.-E.; Vincken, J.-P.; Zheng, C.; Gruppen, H. Diversity of (dihydro) hydroxycinnamic acid conjugates in Columbian potato tubers. *Food Chem.* **2013**, *139*, 1087–1097.
- (12) Shakya, R.; Navarre, D. A. LC-MS analysis of solanidane glycoalkaloids diversity among tubers of four wild potato species and three cultivars (*Solanum tuberosum*). *J. Agric. Food Chem.* **2008**, *56*, 6949–6958.
- (13) Yang, M.; Bernards, M. A. Wound-induced metabolism in potato (*Solanum tuberosum*) tubers. *Plant Sig. Behav.* **2006**, *1*, 59–66.
- (14) Yang, W.-L.; Bernards, M. A. Metabolite profiling of potato (*Solanum tuberosum* L.) tubers during wound-induced suberization. *Metabol.* **2007**, *3*, 147–159.
- (15) Reyes, L. F.; Cisneros-Zevallos, L. C. Wounding stress increases the phenolic content and antioxidant capacity of purple-flesh potatoes (*Solanum tuberosum* L.). *J. Agric. Food Chem.* **2003**, *51*, 5296–5300.
- (16) Reyes, L. F.; Villarreal, J. E.; Cisneros-Zevallos, L. The increase in antioxidant capacity after wounding depends on the type of fruit or vegetable tissue. *Food Chem.* **2007**, *101*, 1254–1262.
- (17) Re, R.; Pellegrini, N.; Pannala, A.; Yang, M.; Rice-Evans, C. Antioxidant activity applying an improved ABTS radical cation decolorization assay. *Free Radical Biol. Med.* **1999**, *26*, 1231–1237.
- (18) Ji, X.; Rivers, L.; Zielinski, Z.; Xu, M.; MacDougall, E.; Stephen, J.; Zhang, S.; Wang, Y.; Chapman, R. G.; Keddy, P.; Robertson, G. S.; Kirby, C. W.; Embleton, J.; Worrall, K.; Murphy, A.; De Koeyer, D.; Tai, H.; Yu, L.; Charter, E.; Zhang, J. Quantitative analysis of phenolic components and glycoalkaloids from 20 potato clones and in vitro evaluation of antioxidant, cholesterol uptake, and neuroprotective activities. *Food Chem.* **2012**, *133*, 1178–1187.
- (19) Nara, K.; Miyoshi, T.; Honma, T.; Koga, H. Antioxidant activity of bound-form phenolics in potato peels. *Biosci. Biotechnol. Biochem.* **2006**, *70*, 1489–1491.
- (20) Kim, H. K. C.; Y, H.; Verpoorte, R. NMR-based metabolomics analysis of plants. *Nat. Protoc.* **2010**, *5*, 536–549.
- (21) Choi, H.-K.; Choi, Y. H.; Verberne, M.; Lefeber, A. W. M.; Erkelens, C.; Verpoorte, R. Metabolic fingerprinting of wild type and transgenic tobacco plants by <sup>1</sup>H NMR and multivariate analysis technique. *Phytochemistry* **2004**, *65*, 857–864.
- (22) Navarre, D. A.; Pillai, S. S.; Shakya, R.; Holden, M. J. HPLC profiling of phenolics in diverse potato genotypes. *Food Chem.* **2011**, *127*, 34–41.
- (23) Katajamaa, M.; Miettinen, J.; Orešič, M. MZmine: Toolbox for processing and visualization of mass spectrometry based molecular profile data. *Bioinformatics* **2006**, *22*, 634–636.
- (24) King, R. R.; Calhoun, L. A. Characterization of cross-linked hydroxycinnamic acid amides isolated from potato common scab lesions. *Phytochemistry* **2005**, *66*, 2468–2473.
- (25) Back, K. Hydroxycinnamic acid amides and their possible utilization for enhancing agronomic traits. *Plant Pathology J.* **2001**, *17*, 123–127.
- (26) King, R. R.; Calhoun, L. A. A feruloyltyramine trimer isolated from potato common scab lesions. *Phytochemistry* **2010**, *71*, 2187–2189.
- (27) Cornelius, M. T. F.; de Carvalho, M. G.; da Silva, T. M. S.; Alves, C. C. F.; Siston, A. P. N.; Alves, K. Z.; Sant'Anna, C. M. R.; Neto, M. B.; Eberlin, M. N.; Braz-Filho, R. Other chemical constituents isolated from *Solanum crinitum* Lam. (Solanaceae). *J. Braz. Chem. Soc.* **2010**, *21*, 2211–2219.
- (28) Bernards, M. A. Demystifying suberin. *Can. J. Bot.* **2002**, *80*, 227–240.
- (29) Graca, J.; Santos, S. Suberin: A biopolyester of plant's skin. *Macromol. Biosci.* **2007**, *7*, 128–135.
- (30) Savarese, S.; Andolfi, A.; Cimmino, A.; Carputo, D.; Frusciant, L.; Evidente, A. Glycoalkaloids as biomarkers for recognition of cultivated, wild and somatic hybrids of potato. *Chem. Biodiver.* **2009**, *6*, 437–446.
- (31) Valcarcel, J.; Reilly, K.; Gaffney, M.; O' Brien, N. Effect of genotype and environment on the glycoalkaloid content of rare, heritage and commercial potato varieties. *J. Food Sci.* **2014**, *79*, T1039–T1048.
- (32) Milner, S. E.; Brunton, N. P.; Jones, P. W.; O' Brien, N. M.; Collins, S. G.; Maguire, A. R. Bioactivities of glycoalkaloids and their aglycones from *Solanum tuberosum*. *J. Agric. Food Chem.* **2011**, *59*, 3454–3484.
- (33) Bassard, J.-E.; Ulmann, P.; Bernier, F.; Werck-Reichhart, D. Phenolamides: Bridging polyamine to the phenolic metabolism. *Phytochemistry* **2010**, *71*, 1808–1824.
- (34) Halket, J. M.; Waterman, D.; Przyborowska, A. M.; Patel, R. K. P.; Fraser, P. D.; Bramley, P. M. Chemical derivatization and mass spectral libraries in metabolite profiling by GC/MS and LC/MS/MS. *J. Exp. Bot.* **2005**, *56*, 219–243.
- (35) van der Kooy, F.; Maltese, F.; Choi, Y. H.; Kim, H. K.; Verpoorte, R. Quality control of herbal material and phytopharmaceuticals with MS and NMR based metabolic fingerprinting. *Planta Med.* **2009**, *75*, 763–775.
- (36) Robinette, S.; Zhang, F.; Bruschweiler-Li, L.; Bruschweiler, R. Web server based complex mixture analysis by NMR. *Anal. Chem.* **2008**, *80*, 3606–3611.
- (37) Magalhaes, L. M.; Segundo, M. A.; Reis, S.; Lima, J. L. F. C. Methodological aspects about in vitro evaluation of antioxidant properties. *Anal. Chim. Acta* **2008**, *613*, 1–19.
- (38) Prior, R. L.; Wu, X.; Schaich, K. Standardized methods for the determination of antioxidant capacity and phenolics in foods and dietary supplements. *J. Agric. Food Chem.* **2005**, *53*, 4290–4302.
- (39) Shafek, R. E.; Shafik, N. H.; Michael, H. N. Antibacterial and antioxidant activities of two new kaempferol glycosides isolated from *Solenostemma argel* stem extract. *Asian J. Plant Sci.* **2012**, *11*, 143–147.
- (40) Amakura, Y.; Yoshimura, M.; Yamakami, S.; Yoshida, T. Isolation of phenolic constituents and characterization of antioxidant markers from sunflower (*Helianthus annuus*) seed extract. *Phytochem. Lett.* **2013**, *6*, 302–305.
- (41) Hadjipavlou-Litina, D.; Garnelis, T.; Athanassopoulos, C. M.; Papaioannou, D. Kukoamine A analogs with lipoxygenase inhibitory activity. *J. Enz. Inhib. Med. Chem.* **2009**, *24*, 1188–1193.
- (42) Mozdzan, M.; Szmraj, J.; Rysz, J.; Stolarek, R. A.; Nowak, D. Antioxidant activity of spermine and spermidine re-evaluated with oxidizing systems involving iron and copper ions. *Int. J. Biochem. Cell B* **2006**, *38*, 69–81.
- (43) Madiwale, G. P.; Reddivari, L.; Stone, M.; Holm, D. G.; Vanamala, J. Combined effects of storage and processing on the bioactive compounds and pro-apoptotic properties of color-fleshed potatoes in human colon cancer. *J. Agric. Food Chem.* **2012**, *60*, 11088–11096.
- (44) Morris, S. C.; Forbes-Smith, M. R.; Scriven, F. M. Determination of optimum conditions for suberization, wound periderm formation, cellular desiccation and pathogen resistance in



wounded *Solanum tuberosum* tubers. *Physiol. Mol. Plant P.* **1989**, *36*, 177–190.

(45) Wu, S.-B.; Meyer, R. S.; Withaker, B. D.; Litt, A.; Kennelly, E. J. A new liquid chromatography-mass spectrometry based strategy to integrate chemistry, morphology, and evolution of eggplant species. *J. Chrom. A* **2013**, *1314*, 154–172.

(46) Matsuda, F.; Morino, K.; Ano, R.; Kuzawa, M.; Wakasa, K.; Miyagawa, H. Metabolic flux analysis of the phenylpropanoid pathway in elicitor-treated potato tuber tissue. *Plant Cell Physiol.* **2005**, *46*, 454–466.

(47) Clifford, M. N.; Wu, W.; Kirkpatrick, J.; Jaiswal, R.; Kunhnert, N. Profiling and characterization by liquid chromatography/multi-stage mass spectrometry of the chlorogenic acids in *Gardeniae fructus*. *Rapid Commun. Mass Sp.* **2010**, *24*, 3109–3120.

(48) Panusa, A.; Zuorro, A.; Lavecchia, R.; Marrosu, G.; Petrucci, R. Recovery of natural antioxidants from spent coffee grounds. *J. Agric. Food Chem.* **2013**, *61*, 4162–4168.

(49) Jaiswal, R.; Matei, M. F.; Golon, A.; Witt, M.; Kunhnert, N. Understanding the fate of chlorogenic acids in coffee roasting using mass spectrometry based targeted and non-targeted analytical strategies. *Food Funct.* **2013**, *3*, 976–984.

(50) Gomez-Romero, M.; Segura-Carretero, A.; Fernandez-Gutierrez, A. Metabolite profiling and quantification of phenolic compounds in methanol extracts of tomato fruit. *Phytochemistry* **2010**, *71*, 1848–1864.

(51) Mader, J.; Harshadrai, R.; Kroh, L. W. Composition of phenolic compounds and glycoalkaloids  $\alpha$ -Solanine and  $\alpha$ -Chaconine during commercial potato processing. *J. Agric. Food Chem.* **2009**, *57*, 6292–6297.